Journal of Nuclear Materials 379 (2008) 169–173

Contents lists available at ScienceDirect

Journal of Nuclear Materials

journal homepage: www.elsevier.com/locate/jnucmat

# Failure model and Monte Carlo simulations for titanium (grade-7) drip shields under Yucca Mountain repository conditions

Z. Qin *, D.W. Shoesmith

*Department of Chemistry, The University of Western Ontario, London, Ontario, Canada N6A 5B7*

ARTICLE INFO

*PACS:*
82.45.Bb
82.20.Wt
02.70.Uu

ABSTRACT

A failure model was developed for the titanium alloy drip shield proposed for the Yucca Mountain nuclear waste repository. The degradation modes considered are hydrogen-induced cracking (HIC) and general aqueous corrosion, processes which are inextricably linked. Failure by HIC is controlled by the environment, the corrosion rate, the material properties, and the hydrogen absorption efficiency which is assumed to decrease parabolically with time. This model includes both oxygen and water reduction coupled to corrosion, and allows for the release of the absorbed hydrogen as the alloy containing the hydrogen converts to oxide. Monte Carlo simulations were employed to predict drip shield lifetimes, and to investigate the effects of the hydrogen absorption efficiency, the critical HIC concentration, the corrosion rate, and the fraction of corrosion supported by water reduction, on the susceptibility of the material to HIC.



## 1. Introduction

The engineered barriers system (EBS) proposed for the high level radioactive waste repository at Yucca Mountain (Nevada, USA) is a combination of a Ni–Cr–Mo alloy waste package (WP) and a Ti alloy (Ti-7 for the shell, and T-28 and -29 for the support members) drip shield (DS). While the WP is the primary barrier to radionuclide release, the DS will divert potential seepage water and rock-fall impingement from the WP. The primary function of the DS is to protect the WP from seepage drips that could lead to crevice corrosion during the early emplacement period when evaporative processes could produce deliquescent deposits and the establishment of aqueous conditions at temperatures well above 100 °C [1].

The selection of Ti alloys for the fabrication of the DS is because of their exceptional resistance to general aqueous corrosion (GC). However, Ti alloys are potentially susceptible to hydrogen-induced cracking (HIC) as a consequence of H absorbed during GC [2]. Enhanced hydrogen absorption could occur if Ti was subjected to a short period of crevice corrosion [3], but this is not expected for the Pd-containing or Ru-containing α-alloys proposed for DS fabrication [4–6]. It has been clearly demonstrated that the accumulation of crevice corrosion damage in these materials requires $T \geqslant 200$ °C. Since the Yucca Mountain repository would be an open, unpressurized system, aqueous conditions are impossible at such temperatures.

Previously, we have developed a failure model for the DS assuming hydrogen absorption only occurs under GC conditions [7]. This model assumes that a constant fraction of the H produced due to anoxic corrosion (i.e. sustained by water reduction only) is absorbed into the alloy eventually leading to HIC once the H concentration in the alloy exceeds a critical value, $C_{HIC}$. Hydrogen absorption into the titanium was assumed to occur via H transport within the defective surface oxide film. While such a process is unlikely in the absence of cathodic polarization or galvanic coupling to a reactive metal, it was adopted as a conservative approach to analyzing possible failure. The basis of this mechanism has been discussed elsewhere [8]. This model predicted all failures were inevitably caused by HIC, but contained conservative features not entirely consistent with available evidence.

1. The hydrogen absorption efficiency ($f_H$) was assumed constant and the values adopted were based on measurements performed under cathodically polarized conditions; i.e. at potentials considerably more negative than achievable under repository conditions. In addition, experimental evidence [9–11] exists to show that $f_H$ decreases with time as surface absorption sites become saturated and the oxide film, a transport barrier to hydrogen, thickens.
2. Corrosion was assumed to be sustained by the H-producing water reduction reaction only, despite the fact conditions within the repository should be indefinitely aerated. Thus, corrosion would be sustained by both oxygen (1a) and water (1b) reduction

$$O_2 + 2H_2O + 4e^- \rightarrow 4OH^-, \quad (1a)$$

$$2H_2O + 2e^- \rightarrow H_2 + 2OH^-, \quad (1b)$$

* Corresponding author. Tel.: +1 519 661 2111x86219; fax: +1 519 661 3022.
*E-mail address:* zqin@uwo.ca (Z. Qin).

0022-3115/$ - see front matter © 2008 Elsevier B.V. All rights reserved.
doi:10.1016/j.jnucmat.2008.06.024

which would suppress H production and, hence, limit its absorption into the alloy.

3. The $C_{HIC}$ was determined in slow strain rate experiments, as the threshold value above which slow crack growth is no longer observed and only fast crack growth occurs. Failure by fast crack growth is not inevitable at $C_{HIC}$, but the possibility of fast failure increases once the critical value is exceeded. Effectively, $C_{HIC}$ defines the material's susceptibility to HIC, and to assume failure is then immediate is to ignore crack growth kinetics. However, it has been pointed out that this critical H concentration may depend on the experimental strain rate used [12], and, hence, the values obtained cannot be considered absolute values.

The model presented here has been revised to account for these additional features. Besides allowing for the release of the absorbed H, as in the previous version of the model [7], the $f_H$ is assumed to decrease parabolically with time, in an attempt to incorporate the influence of saturation of available H absorption sites. Monte Carlo simulations are then employed to investigate the influence of $f_H$, $C_{HIC}$, corrosion rate ($R_{GC}$), and the fraction of the corrosion process supported by water reduction ($\varepsilon$), on susceptibility of the material to HIC and how this influences DS performance.

## 2. Mathematical model

It could be argued that support of corrosion by $O_2$ reduction will eliminate the possibility of corrosion support by water reduction, and, hence, hydrogen absorption should not occur at all. However, it has been clearly shown that, for $T \geqslant 70$ °C, oxide fracture and repair events can be frequent on Ti-7 leading to corrosion in the grain boundaries of the alloy [13]. Recently, using scanning electrochemical microscopy on the Ti-2 and Ti-7 alloys [14,15], we have demonstrated that these corrosion processes are associated with Fe-stabilized phases (β-phase, and $Ti_xFe/Ti_xFe_yPd_z$ intermetallic precipitations) in the grain boundaries of the alloy. Since localized acidification within grain boundaries will accompany these corrosion events, they will almost certainly involve $H^+$ reduction and the absorption of H. This introduces the possibility that corrosion of grains will be supported by $O_2$ reduction while corrosion in grain boundaries is supported by $H^+$ reduction leading to H absorption, as illustrated schematically in Fig. 1.

If the fraction of the overall corrosion process supported by water reduction is $\varepsilon$, then, at the corrosion potential, the cathodic current densities associated with reactions (1a), $i_{1a}$, and (1b), $i_{1b}$, are related to the anodic Ti corrosion current density, $i_{Ti}$, by the equation

$$i_{1a} = -(1-\varepsilon)\cdot i_{Ti}, \quad i_{1b} = -\varepsilon \cdot i_{Ti}. \tag{2}$$

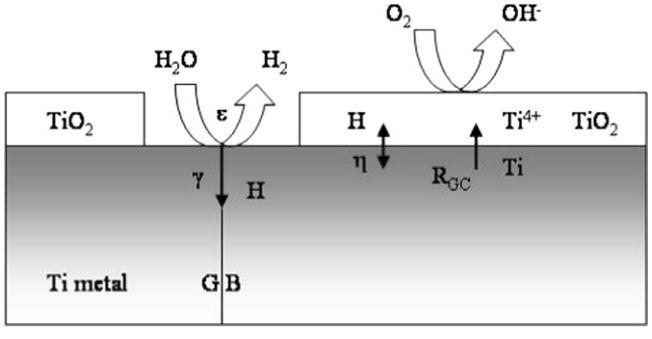


**Fig. 1.** Schematic illustrating the linkage between GC and hydrogen absorption. The symbols are explained in the text.

The amount (moles) of H absorbed ($m_{in}$) in an infinitesimal period of time is given by

$$dm_{in} = \rho_{Ti} A \varepsilon \gamma (1 - C_H) R_{GC} dt, \tag{3}$$

where $A$ is the area, $\rho_{Ti}$ is the density of Ti, $R_{GC}$ is the corrosion rate, and $\gamma$, the hydrogen absorption factor, is related to the fractional hydrogen absorption efficiency $f_H$ by $\gamma = 4f_H/M_{Ti}$, where $M_{Ti}$ is the atomic weight of Ti. The portion of the penetration volume composed of already absorbed H is not included in Eq. (3) since it will not contribute to the generation of H by reaction (1b). The H concentration by weight, $C_H$, is defined for a uniform H distribution (implicitly assuming the absorbed H is rapidly dispersed throughout the remaining alloy) as

$$C_H(t) = \frac{m_H(t)}{\rho_{Ti} A (h_0 - R_{GC} t)}, \tag{4}$$

where $m_H$ is the amount of H in the remaining alloy, and $h_0$ is the original wall thickness. While $m_H$ is an extensive quantity, $C_H$ is an intensive quantity, and, thus, not accumulative. While rapid dispersion in this manner is unlikely, it remains a conservative assumption while evidence on which to base a more realistic model remains elusive.

When the alloy corrodes, the H already contained in the alloy could be released to the oxide. There is also the possibility of a re-distribution of H between the alloy and the oxide, which would effectively reduce the amount of H being released from the volume of alloy consumed by corrosion. Therefore, the loss of H ($m_{out}$) is given by

$$dm_{out} = \rho_{Ti} A (1 - \eta) C_H R_{GC} dt, \tag{5}$$

where $\eta$ is the factor for the portion of the H that is not released when the alloy converts to oxide. It has been demonstrated that calculations are insensitive to the value of $\eta$ unless $C_H$ is far in excess of $C_{HIC}$ [7]. For simplicity $\eta = \varepsilon\gamma$ is assumed in the following derivations.

The net hydrogen absorption rate ($dm_H = dm_{in} - dm_{out}$) can thus be obtained from Eqs. (3) to (5)), as

$$\frac{dm_H(t)}{dt} + \frac{m_H(t)}{(t_{GC} - t)} = \rho_{Ti} A R_{GC} \varepsilon \gamma, \tag{6}$$

where $t_{GC} = h_0/R_{GC}$ is the time when the full wall thickness, $h_0$, is penetrated by GC. In the previous model [7], $\gamma$ was assumed to be a constant. Here, $\gamma$ (or $f_H$) is assumed to decrease parabolically with time, i.e.

$$\gamma(t) = \gamma_0/\sqrt{t}, \tag{7}$$

where $\gamma_0 = 4f_H^0/M_{Ti}$ is a constant and $f_H^0$ is the hydrogen absorption efficiency constant. Eq. (6) is a first order linear differential equation that can be solved to give

$$m_H(t) = \rho_{Ti} A R_{GC} \varepsilon \gamma_0 \frac{(t_{GC} - t)}{\sqrt{t_{GC}}} \ln\left[\frac{\sqrt{t_{GC}} + \sqrt{t}}{\sqrt{t_{GC}} - \sqrt{t}}\right] \tag{8}$$

and via Eq. (4)

$$C_H(t) = \frac{\varepsilon\gamma_0}{\sqrt{t_{GC}}} \ln\left[\frac{\sqrt{t_{GC}} + \sqrt{t}}{\sqrt{t_{GC}} - \sqrt{t}}\right]. \tag{9}$$

The evolution of $m_H(t)$ and $C_H(t)$ with normalized time ($t/t_{GC}$) are shown in Fig. 2.

The DS will fail by HIC if the H content of the alloy exceeds $C_{HIC}$. The time when $C_H = C_{HIC}$ is given by

$$t_{HIC} = t_{GC} \tanh^2(1/2\beta), \tag{10}$$

where $\beta$, the so-called HIC susceptibility factor, is defined by

$$\beta = \frac{\varepsilon\gamma_0}{C_{HIC}} \sqrt{\frac{R_{GC}}{h_0}}. \tag{11}$$

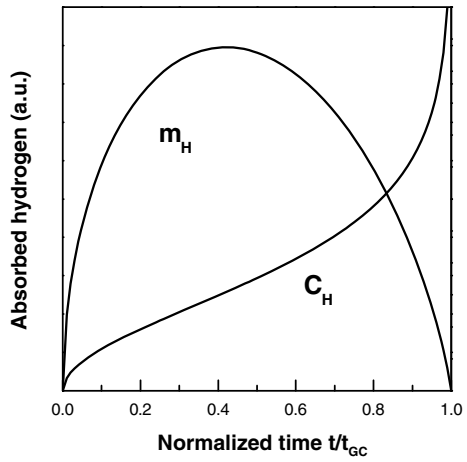


**Fig. 2.** Evolution of $m_H$ and $C_H$ determined from Eqs. (8) and (9).

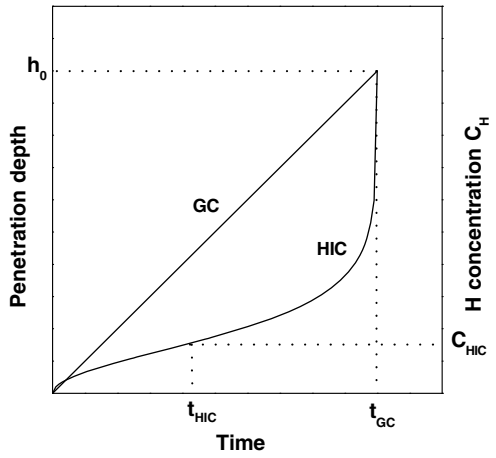


**Fig. 3.** Schematic showing the pathways to, and criteria for, failure by GC and HIC.

As an indicator of the susceptibility to HIC, the higher the value of $\beta$, the more susceptible is the DS to failure by HIC.

The pathways to failure, and the criteria for failure, are illustrated in Fig. 3. Since GC is the source of H leading to hydrogen absorption, the two failure processes are inextricably linked. Failure by HIC will be controlled by the rate of GC ($R_{GC}$), the susceptibility of the alloy to HIC ($C_{HIC}$), the rate of hydrogen absorption ($\gamma_0$), and the fraction of the overall corrosion process supported by proton reduction ($\varepsilon$) in grain boundaries. Both $\gamma_0$ and $\varepsilon$ will depend on the properties of the alloy, especially the distribution of Pd and the impurity Fe in grain boundaries.

## 3. Monte Carlo code – *EBSPA*

The assessment of DS performance in a nuclear waste repository requires predictions over long-times based on experimental databases measured over short times. The resulting uncertainties are generally accounted for by using probabilistic distributions instead of determinate parameter values. The use of such distributions in long-time predictions makes Monte Carlo simulation an ideal tool. A Monte Carlo simulation code (*EBSPA*), currently in its fourth version, was developed to calculate the cumulative probability of failures (CPF) of the EBS. The details of *EBSPA* have been described elsewhere [16]. Here, only the section developed to predict DS performance is utilized.

Corrosion is assumed to commence when the temperature is below a value, $T_{aq}$, the temperature that defines the earliest time for the establishment of aqueous conditions on DS surfaces. The value of $T_{aq}$ depends on the nature of the deliquescent solids formed on the DS due to the evaporation of seepage drips, and the higher $T_{aq}$ the more aggressive the environment. The DS will fail either by HIC, if the H concentration exceeds $C_{HIC}$, or by GC if corrosion damage penetrates the wall allowance, whichever occurs first. The GC and HIC simulation pathways for the DS section of *EBSPA* are outlined in Fig. 4.

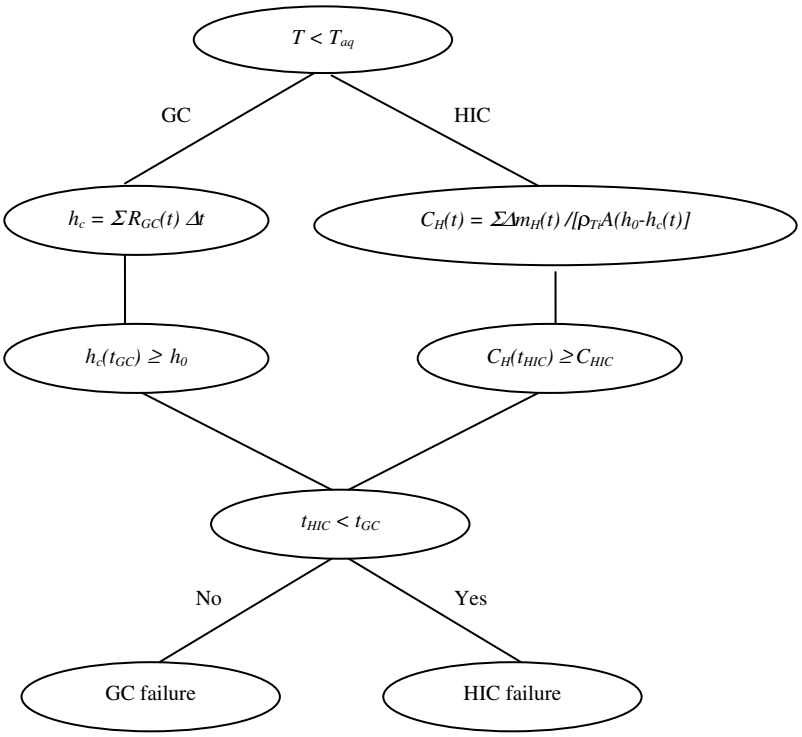


**Fig. 4.** The simulation pathways for the DS section of the *EBSPA* code.

## 4. Simulation results and discussion

Simulations were performed to study the influence of $\varepsilon$, $\gamma_0$ (or $f_H^0$), $C_{HIC}$, and $R_{GC}$ on DS performance under anticipated repository conditions. The values of the parameters used in the simulations are listed in Tables 1 and 2. The simulations usually take 2 h of CPU time for one million realizations.

**Table 1**
Simulation parameters

| Parameter | Distribution | Values |
|---|---|---|
| $d_0$ (m) | N/A | 0.015 |
| $T_{aq}$ (°C) | Determinate | 120 |
| $\varepsilon$ | Uniform | 0–1, 0–0.5, 0–0.1 |
| $R_{GC}$ (scale factor) | Weibull | 22.4566 |
| $R_{GC}$ (shape factor) | Weibull | 0.8057 |
| $R_{GC}$ enhancement | Determinate | *x*1, *x*2, *x*3 |
| $C_{HIC}$ (ppm w) | Uniform | 100–300, 200–600 |
| $f_H^0$ | Uniform | Table 2 |

**Table 2**
$f_H^0$ values in simulations

| Max $f_H^0$ | 0.1 | 0.3 | 0.5 | 0.7 | 0.9 |
|---|---|---|---|---|---|
| $T < 100$ °C | 0.001–0.01 | 0.01–0.1 | 0.1–0.3 | 0.3–0.5 | 0.5–0.7 |
| $T > 100$ °C | 0.01–0.1 | 0.1–0.3 | 0.3–0.5 | 0.5–0.7 | 0.7–0.9 |

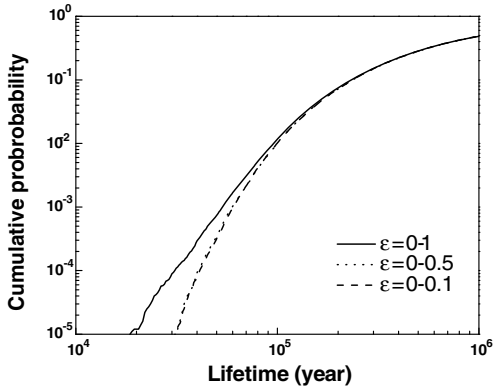


**Fig. 5.** Effect of the fraction of water reduction on DS lifetimes simulated for the conditions: $T_{aq}$ = 120 °C, $C_{HIC}$ = 100–300 ppm, $f_H^0$(<100 °C) = 0.1–0.3, $f_H^0$(>100 °C) = 0.3–0.5, and $R_{GC} \times 1$.

The fraction of corrosion supported by water reduction, $\varepsilon$, is assumed to be uniformly distributed between 0 and a maximum value. This simulation was performed with $T_{aq}$ = 120 °C, which represents a realistic temperature for the onset of aqueous conditions, but with a very conservative range of values for $C_{HIC}$. The choice of this range of values reflects the concerns expressed that slow strain rate tests may not produce unequivocable values for $C_{HIC}$. Fig. 5 shows that the effect of $\varepsilon$ is significant only for early failures, and that the cases $0 \leqslant \varepsilon \leqslant 0.5$ and $0 \leqslant \varepsilon \leqslant 0.1$ have little difference under the conditions simulated.

Fig. 6(a) shows the time of initial failure as a function of $f_H^0$, the initial hydrogen absorption efficiency, for a very conservative range of $C_{HIC}$ values (100–300 ppm) and a more realistic range (200–600 ppm). Since there will be approximately 10000 DS's in the repository, a CPF = $10^{-4}$ can be considered to represent this time to initial failure. Small values of $f_H^0$ have little influence on the time of initial failure, since the failures are primarily by GC rather than by HIC, as illustrated in Fig. 6(b) which shows the fraction of DS failures due to HIC as a function of $f_H^0$. Also shown as numbers in Fig. 6(b) are the values of the HIC susceptibility factor, $\beta$, for each calculation.

These calculations show that HIC only becomes a significant failure mode for $f_H^0 > 0.3$ even for the conservative range of $C_{HIC}$ values. For a more realistic range of $C_{HIC}$ values, failures by HIC become almost insignificant for $f_H^0 < 0.5$. Presently, values for $f_H^0$ are not known. It is possible that an absorption efficiency approaching 1 could prevail initially since absorption in acidified grain boundary locations will initially occur rapidly as demonstrated in galvanostatic charging experiments [17]. However, the immediate formation of surface hydrides will lead to a rapid decrease in absorption efficiency [17], and the rate of hydrogen absorption should adopt the parabolic form assumed in the calculations.

The $R_{GC}$ values used in the simulations are based on values measured, by weight loss, in the Long Term Corrosion Test Facility (LTCTF) at Lawrence Livermore National Laboratory (LLNL) in repository relevant environments, and are fitted to Weibull distributions. The values are in the range 0–78 nm/year with over 80% of measured rates being $\leqslant$30 nm/year. The measurement of such small rates by a technique such as the measurement of weight change leaves some uncertainty over their reliability. To assess whether this is an importance feature, the results of the simulations in which the corrosion rates were multiplied by factors of 2

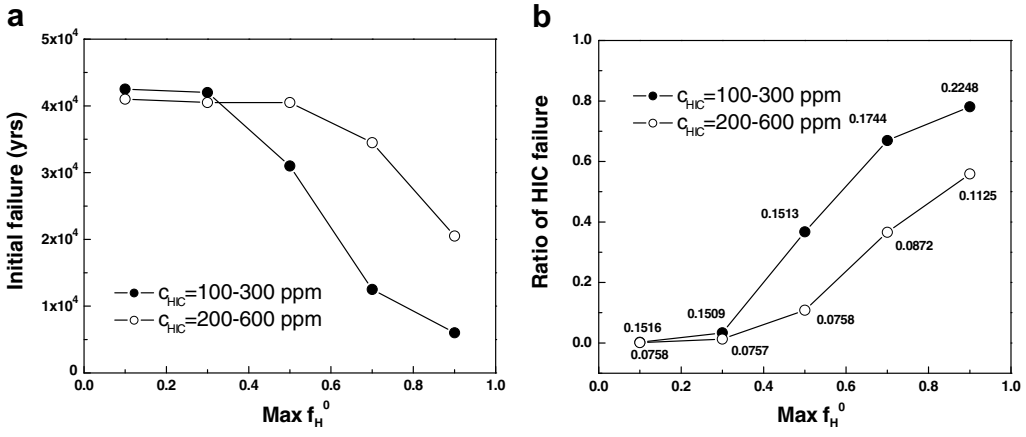


**Fig. 6.** The influences of $f_H^0$ (shown on the *x*-axis as the maximum $f_H^0$) and $C_{HIC}$ on (a) The time of initial DS failure (CPF = $10^{-4}$); (b) The fraction of DS failures due to HIC. The individual values of the HIC susceptibility factor are also shown. (Other simulation conditions: $T_{aq}$ = 120 °C, $\varepsilon$ = 0–1, $R_{GC} \times 1$.)

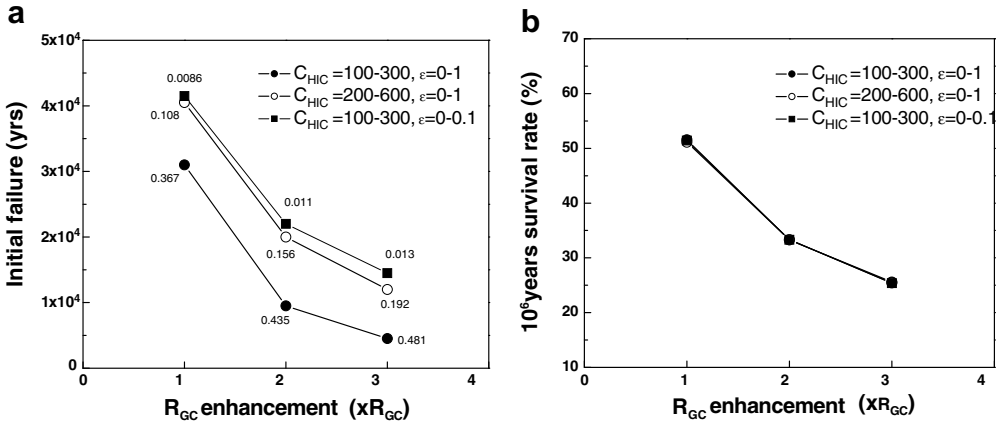


**Fig. 7.** Effect of the enhancement of GC rate on DS lifetimes simulated for the conditions: $T_{aq}$ = 120 °C, $f_H^0$(<100 °C) = 0.1–0.3, $f_H^0$( > 100 °C) = 0.3–0.5. (a) The time of initial DS failure (CPF = $10^{-4}$). The individual values of the fraction of failures due to HIC are also shown. (b) The survival rate of the DS after 1 000 000 years (all points almost coincide).

and 3 are shown in Fig. 7. The calculations show that the $R_{GC}$ has a significant impact on both the initial failure, Fig. 7(a), and the long-time survival rate, expressed as the probability of DS survival to >$10^6$ years Fig. 7(b). This sensitivity arises because $R_{GC}$ affects both GC and HIC. However, the $C_{HIC}$ and $\varepsilon$ values, which affect HIC but not GC, influence only the initial failure, not the long-time survival rate.

## 5. Conclusions and further work

A failure model has been developed incorporating two feasible corrosion processes, GC and HIC, which could lead to failure of the DS under anticipated repository conditions. The failure of the DS is controlled by the environment, the corrosion rate, the material properties, and the hydrogen absorption efficiency which depends on the properties of the oxide film on the alloy surface. While allowing for the release of the absorbed H, this model incorporates both oxygen and water reduction as feasible cathodic reactions able to sustain corrosion, and assumes $f_H$ will decrease parabolically with time. Monte Carlo simulations have been employed to investigate the influence of $\varepsilon$, $\gamma_0$ (or $f_H^0$), $C_{HIC}$, and $R_{GC}$ on the susceptibility of the alloy to HIC and on DS performance. The calculations suggest that HIC is an important mode causing early DS failures, and, hence, should be included in any model for DS performance assessment.

Further improvements to the model will include, but are not limited, to the following:

1. Hydrogen absorption could occur locally at fault sites in the passive film; i.e., grain boundary mismatches, locations of impurity-stabilized phases. Presently, the influence of such features is not well documented.
2. The influence of the enrichment of H near the DS surface, which then tends to be released as corrosion proceeds.
3. The assessment of galvanic coupling between the titanium surface and carbon steel structural components within the repository. Such a coupling would be expected to accelerate the rate of H production and absorption.

## Acknowledgements

The temperature profile and GC rates were provided by Y. Sun (Lawrence Livermore National Laboratories) and F. Hua (Bechtel SAIC Company), respectively.

## References

[1] Z. Qin, D.W. Shoesmith, Mater. Res. Soc. Proc. 824 (2004) 11.
[2] F. Hua, K. Mon, P. Pasupathi, G.M. Gordon, D.W. Shoesmith, Corrosion 61 (2005) 987.
[3] D.W. Shoesmith, J.J. Noel, D. Hardie, B.M. Ikeda, Corros. Rev. 18 (2000) 331.
[4] R.W. Schutz, M. Xiao, in: Proceedings of 12th International Corrosion Congress, vol. 3A, Houston, Texas, 19–24 September 1993, p. 1213.
[5] R.W. Schutz, Platinum Metal Rev. 40 (1996) 54.
[6] F. Hua, K. Mon, P. Pasupathi, G.M. Gordon, D.W. Shoesmith, Corrosion 2004, Paper No. 04689, NACE, Houston, Texas, 2004.
[7] Z. Qin, L. Yan, D.W. Shoesmith, in: Proceedings of International Topical Meeting on Probabilistic Safety Analysis, San Francisco, CA, 11–15 September 2005, p. 399.
[8] F. Hua, K. Mon, P. Pasupathi, G. Gordon, D.W. Shoesmith, J. Metals (2005) 20.
[9] I.I. Phillips, P. Poole, L.L. Shreir, Corros. Sci. 12 (1972) 855; ibid 14 (1974) 533.
[10] R.W. Schutz, Corrosion 97, Paper No. 32, NACE, Houston, Texas, 1997.
[11] H. Tomari, T. Masugata, K. Shimogori, T. Nishimura, R. Wada, N. Taniguchi, Zairyo-to-Kankyo 48 (1999) 807.
[12] Y.-M. Pan, C.S. Brossia, G.A. Cragnolino, D.S. Dunn, G,D. Gute, L. Yang, CNWRA Report 2003-02, Center for Nuclear Waste Regulatory Analyses, San Antonio Texas, 2003.
[13] X. He, J.J. Noel, D.W. Shoesmith, Corrosion 63 (2007) 781.
[14] R. Zhu, C. Nowierski, Z. Ding, J.J. Noel, D.W. Shoesmith, Chem. Mater. 19 (2007) 2533.
[15] R. Zhu, Z. Qin, J.J. Noel, D.W. Shoesmith, Z. Ding, Anal. Chem. 80 (2008) 1437.
[16] Z. Qin, D.W. Shoesmith, Mater. Res. Soc. Proc. 985 (2006) NN03-06.
[17] L. Yan, S. Ramamurthy, J.J. Noel, D.W. Shoesmith, Electrochim. Acta 52 (2006) 1169.